

Published in final edited form as:

*Exp Eye Res.* 2014 November ; 128: 129–140. doi:10.1016/j.exer.2014.08.016.

## Experimental scleral cross-linking increases glaucoma damage in a mouse model

Elizabeth C. Kimball<sup>1</sup>, Cathy Nguyen<sup>1</sup>, Matthew R. Steinhart<sup>1</sup>, Thao D. Nguyen<sup>2</sup>, Mary E. Pease<sup>1</sup>, Ericka N. Oglesby<sup>1</sup>, Brian C. Oveson<sup>1</sup>, and Harry A. Quigley<sup>1</sup>

<sup>1</sup>Glaucoma Center of Excellence, Wilmer Ophthalmological Institute, Johns Hopkins University, Baltimore, MD USA

<sup>2</sup>the Department of Mechanical Engineering, Johns Hopkins University, Baltimore, MD USA

### Abstract

The purpose of this study was to assess the effect of a scleral cross-linking agent on susceptibility to glaucoma damage in a mouse model. CD1 mice underwent 3 subconjunctival injections of 0.5 M glyceraldehyde (GA) in 1 week, then had elevated intraocular pressure (IOP) induced by bead injection. Degree of cross-linking was measured by enzyme-linked immunosorbent assay (ELISA), scleral permeability was measured by fluorescence recovery after photobleaching (FRAP), and the mechanical effects of GA exposure were measured by inflation testing. Control mice had buffer injection or no injection in 2 separate glaucoma experiments. IOP was monitored by Tonolab and retinal ganglion cell (RGC) loss was measured by histological axon counting. To rule out undesirable effects of GA, we performed electroretinography and detailed histology of the retina. GA exposure had no detectable effects on RGC number, retinal structure or function either histologically or electrophysiologically. GA increased cross-linking of sclera by 37% in an ELISA assay, decreased scleral permeability (FRAP,  $p = 0.001$ ), and produced a steeper pressure—strain behavior by in vitro inflation testing. In two experimental glaucoma experiments, GA-treated eyes had greater RGC axon loss from elevated IOP than either buffer-injected or control eyes, controlling for level of IOP exposure over time ( $p = 0.01$ , and  $0.049$ , multivariable regression analyses). This is the first report that experimental alteration of the sclera, by cross-linking, increases susceptibility to RGC damage in mice.

### Keywords

glaucoma; sclera; mouse; retinal ganglion cell; extracellular matrix; collagen; cross-linking; glyceraldehyde

---

© 2014 Elsevier Ltd. All rights reserved.

Correspondence: Elizabeth Cone Kimball, Smith Building M002, Wilmer Eye Institute, Johns Hopkins University, 400 North Broadway, Baltimore, MD USA 21287; telephone: +1 410 955 3337; fax: +1 443 287 2711; fcone1@jhmi.edu.

**Publisher's Disclaimer:** This is a PDF file of an unedited manuscript that has been accepted for publication. As a service to our customers we are providing this early version of the manuscript. The manuscript will undergo copyediting, typesetting, and review of the resulting proof before it is published in its final citable form. Please note that during the production process errors may be discovered which could affect the content, and all legal disclaimers that apply to the journal pertain.

## 1. Introduction

Glaucoma is the second leading cause of blindness worldwide (Quigley and Broman, 2006), and the incidence and progression of open angle glaucoma (OAG) are closely related to mean intraocular pressure (IOP) (Bengtsson and Heijl, 2005) and to its variability (Nouri-Mahdavi et al., 2004; Boland and Quigley, 2007). IOP acts a mechanical load on the lamina cribrosa through the translaminar pressure differential and the tensile hoop stresses in the sclera. These two effects combine to produce a stress and deformation state that leads to alterations in ONH glial and connective tissues, damage to RGC axons (Quigley et al, 1981), and ultimately to ONH excavation, a defining clinical feature of glaucoma (Quigley et al., 1983; Burgoyne et al., 2005). Histological and physiological evidence suggests that both anterograde and retrograde RGC axonal transport are interrupted soon after a change in IOP from baseline levels, in human eyes (Quigley and Green, 1979), and in monkey (Gaasterland and Kupfer, 1974) and rodent eyes (Morrison et al., 1990).

Mammalian eyes that are subjected to experimental IOP increase have neuronal, glial, and associated tissue alterations that are phenotypically similar to those of human glaucoma (Morrison et al., 1990; Morrison et al., 1997). Furthermore, lowering of IOP protects against progressive worsening of both animal and human glaucoma (Morrison et al., 1998; Heijl et al., 2002). IOP generates stress and strain in the sclera and lamina cribrosa, the level of which depends on the mechanical properties of the tissues. Variation in the mechanical properties of the ocular connective tissues may explain why half of individuals with OAG suffer injury at physiological IOP levels (Quigley and Broman, 2006). Biomechanical models (Norman et al., 2011, Sigal et al. 2005, Girard 2009, Sigal et al. 2011, Coudrillier et al. 2013) suggest that the mechanical behavior of the sclera significantly influences the stress and deformation of the lamina cribrosa (LC) and may be a critical mechanical driver of glaucomatous damage to RGC axons. The candidate genes and their products that affect glaucoma damage may include those determining scleral composition and its response to IOP-related stress. Corneal hysteresis and myopia with its thinner sclera have been implicated as glaucoma risk factors (Boland and Quigley, 2007; Congdon et al., 2006).

Mechanical testing of normal human (Woo et al., 1972, Coudrillier 2012, Fazio 2013), porcine (Girard et al., 2008), monkey (Girard et al., 2009) and rabbit (Greene et al., 1979) scleral tissue established that the sclera deforms nonlinearly in response to IOP elevation and creeps at constant elevated IOP. The structure of the mouse sclera is similar in several respects to that of human sclera (Gelman et al., 2010; Watson and Young, 2004). The sclera becomes thinner with aging (Girard et al. 2009; Coudrillier et al. 2012) and there are decreases with age in decorin, biglycan and elastin (Watson and Young, 2004; Rada et al., 2000). An increase in glycation of collagen fibrils with age may be a factor in increasing their cross-sectional area (Keeley et al., 1984; Malik et al., 1992). Increased mechanical stiffness of the sclera with age has been reported in human (Avetisov et al., 1984; Friberg and Lace, 1988; Coudrillier et al. 2012; Geraghty et al., 2012), monkey (Girard et al., 2009), and mouse (Myers et al., 2010), in part due to increasing intermolecular collagen crosslinking with age (Curtin, 1969; Ihanamaki et al., 2001; Girard et al., 2009). Fazio et al. (2013) showed that the strains in the peripapillary sclera were significantly lower in older human specimens. The structure of the mouse lamina cribrosa is similar to the human sclera,

in that axon bundles pass out through septae; however, the septae in the mouse consist of astrocytes, not connective tissue beams surrounded by astrocytes as in the monkey and human (Sun et al., 2009).

There is evidence that both human glaucoma and experimental animal models of glaucoma lead to increased scleral stiffness. Downs et al. (2005) showed that the stress relaxation behavior measured by strip tests of monkey sclera with induced glaucoma damage displayed a larger relaxation time and equilibrium modulus compared to the sclera of normal monkey eyes. Nguyen et al., (2013) found increased stiffness in mouse eyes exposed to elevated IOP. Hommer et al., (2008) measured *in vivo* ocular expansion caused by blood pressure pulsation and concluded that the eyes of glaucoma patients exhibited a higher ocular stiffness than those of non-glaucoma patients. Coudrillier et al. (2012) found that human glaucoma eyes were stiffer than normal in *post-mortem* inflation testing. It is critical to determine whether scleral stiffening as observed in human glaucoma eyes is a beneficial adaptation or a detrimental contributor to ONH injury. A stiffer sclera would decrease the expansion of the sclera canal, but would also potentially increase posterior bowing of the LC (Yang et al., 2009).

The aim of this work is to investigate the effect of scleral stiffness on the susceptibility to glaucoma damage. The concept of scleral crosslinking was introduced in 2004 by Wollensak et al. and further elaborated as a potential treatment of progressive myopia. This *in vivo* method (Wollensak et al, 2008a; Wollensak et al, 2008a), was used to increase the stiffness of mouse sclera by subconjunctival injection of 0.5 M glyceraldehyde (GA), a known collagen crosslinking agent (Tessier et al., 2003; Danilov et al., 2008). We measured the alteration in biomechanical behavior caused by GA treatment using an *in vitro* inflation test (Myers et al., 2010) of normal and experimental glaucoma eyes compared to their contralateral controls. Corneal cross-linking treatment has been applied to human eyes with keratoconus, by activating riboflavin with ultraviolet light (Wollensak et al., 2003). Exposure of living rabbit corneas to GA increased cross-linkage and altered stress—strain behavior without significant damage to either the retina or to other ocular structures (Wollensak et al., 2005; Wollensak et al., 2008a; Wollensak et al., 2008b; Wollensak et al., 2009; Mattson et al., 2010; Terai et al., 2012). Cross-linking of sclera in excised pig eyes has shown increased stiffness (Thornton et al., 2009). To our knowledge, this is the first test of the effect of an experimental scleral modification on glaucoma damage.

## 2. Methods

### 2.1. Mice

We used 381 CD1 albino, female mice that were 2 months of age at the start of experiments (Charles River, Inc., Wilmington, MA). Animals were treated in accordance with the ARVO Statement for the Use of Animals in Ophthalmic and Vision Research. All protocols were approved and monitored by the Johns Hopkins University School of Medicine Animal Care and Use Committee. For individual study breakdown, please see Table 2.

## 2.2. GA Exposure

Mice were anesthetized with a mixture of ketamine (Fort Dodge Animal Health, Fort Dodge, IA), xylazine (VedCo Inc., Saint Joseph, MO), and acepromazine (Phoenix Pharmaceuticals, Burlingame, CA) at 50, 10 and 2 mg/kg, respectively. The dosage and time of anesthesia was controlled and has been standardized as previously published (Cone et al., 2010, Gelman et al., 2010, Nguyen et al., 2013, Cone-Kimball., 2013). There is no reason to believe that variation in anesthesia was a factor in the comparative IOP data within animals or across groups of animals. Investigators were masked during injection to the content of the injected material, masked during IOP measurements after bead injection, and masked during all data acquisition including axon loss assessment. The GA experimental and control animals were treated in masked fashion on the same days, interchangeably, so that any difference in the state or effect of anesthesia would be random and would not lead to any systematic bias. A pilot opening was made in the conjunctiva with a 30 gauge needle and injections of GA or buffer were made with a mouse tail vein catheter (SAI Infusion Technologies, Libertyville, IL) connected to a 1 cc syringe. The largest volume that could be injected was 0.4 cc of 0.5 M GA (Sigma-Aldrich, St. Louis, MO, USA) dissolved in 0.1 M phosphate buffer (0.1 M Na<sub>3</sub>PO<sub>4</sub>, pH=7.2). At all steps of the experiment the solutions and tissues were coded to mask the participants. The solutions were slowly injected over 5–10 seconds, the cannula was removed after 1 minute, and excess solution was blotted with a cotton swab. IOP was measured immediately, at 3 days, and at one week. Animals receiving subconjunctival injections had 3 injections of either GA or buffer over a 7 day period- Day 0, Day 3, and Day 7. In glaucoma experiments, elevated IOP was induced by bead injection one week after the third subconjunctival injection. For assessment of GA effects, some eyes received only 1 or 2 GA injections, or lower concentrations of GA (0.1 and 0.3 M). We completed inflation studies on groups of 5–10 animals using these lower concentrations and found that the effects on stiffness in inflation testing were less consistent and insufficient to be statistically significant (data not included). At 0.5 M GA, the stiffening effects after 2 or 3 injections were significant (Figure 2), without causing toxicity. Some effects of GA were also tested by soaking eyes after enucleation in 0.5 M GA for 1–24 hours. Exposure to glutaraldehyde (not glyceraldehyde, a different molecule) in 3 tested concentrations was found to be toxic or lethal (data not shown).

## 2.3. Bead Injection Glaucoma Model

The use of CD1 mouse was decided after having previously published (Cone et al., 2010) that CD1 animals had a greater susceptibility to axon loss than B6. We believed that having a model with greater susceptibility would allow us to better measure the beneficial or detrimental effects of the cross-linking effects of glyceraldehyde exposure. Mice were anesthetized with intraperitoneal injection of ketamine, xylazine, and acepromazine (50, 10 and 2 mg/kg, respectively) and the left anterior chamber was injected with Polybead Microspheres<sup>®</sup> (Polysciences, Inc., Warrington, PA, USA), using the 4+1 protocol (Cone et al., 2010), consisting of 2 µl of 6 µm diameter beads, then 2 µl of 1 µm diameter beads, followed by 1 µl of viscoelastic compound (10 mg/ml sodium hyaluronate, Healon; Advanced Medical Optics Inc., Santa Ana, CA). The injections were made through a glass cannula with 50 µm tip diameter, connected to a Hamilton syringe (Hamilton, Inc., Reno, NV). IOP was measured immediately after injection, and at 3 days, 1 week, 2 weeks and 6

weeks, using the Tonolab tonometer (TioLat, Inc., Helsinki, Finland). For IOP measurements, mice were anesthetized by inhalation of a mixture of oxygen and isoflurane using the RC<sup>2</sup>-Rodent Circuit Controller (VetEquip, Inc., Pleasanton, CA) and received topical anesthesia with 0.5% proparacaine hydrochloride eye drops (Akorn Inc., Buffalo Grove, IL, USA). We have published the accuracy of the Tonolab in normal and glaucoma mice (Pease et al., 2006; Pease et al., 2011), but to confirm that GA treatment did not affect the accuracy of IOP measurement, we measured IOP in GA-injected eyes of anesthetized mice with IOP set by cannulation and attachment to a reservoir whose height determined the pressure. We collected 5 means of 6 measurements at each IOP setting (a total of 30 measurements per eye) and used the median of 5 means as final IOP. Readings were taken stepwise at reservoir heights corresponding to pressures of 10, 20, 30, 40, and 50 mm Hg. The Tonolab IOP was compared to set IOP by linear regression, with measured  $y = 1.06x + 0.52$ ,  $R^2 = 0.99$  for control eyes and  $y = 1.05x - 0.95$ ,  $R^2 = 0.99$  for GA-injected eyes, indicating accurate representation of set IOP and no difference between groups.

Three sets of mice received 3 injections of GA and 2 of these underwent experimental glaucoma. In one experiment, unilaterally 3x GA-injected mice (N=40) were compared to buffer-injected mice (N=41) and in a second, confirming experiment, 3x GA-injected mice were compared to bilateral controls (N=20). In both groups, the primary outcome was the degree of RGC axon loss. The third set of animals underwent 3 GA injections and were tested for potential effects of the injection on retinal histology (N=5), electroretinography (ERG, N=5), scleral advanced glycation end products concentration (AGE, N=38), and biomechanical behavior (N=157).

#### 2.4. Biomechanical Inflation Testing

Eyes of 4–6 month old CD1 mice were inflation tested *post-mortem* in a procedure previously published (Nguyen et al., 2013) and modified as indicated below. Inflation testing was carried out on eyes that had undergone 6 weeks of elevated IOP after GA (N=31) or buffer injection (N=28), as well as 6 week glaucoma eyes without subconjunctival injection (N=20), control eyes (N=28), eyes that had undergone GA injection alone without glaucoma (N=24), and eyes that were soaked *in vitro* in GA for 5 minutes to 24 hours (N=26). Animals were anesthetized with a mixture of ketamine, xylazine, and acepromazine, the superior cornea was marked for orientation, and the eyes were enucleated and the animal sacrificed by exsanguination. The axial length was measured from the cornea to the temporal optic nerve margin, while width was measured at the largest dimension at the equator, midway between cornea and optic nerve, in both the nasal-temporal axis and the superior—inferior axis with a digital caliper (Instant Read Out Digital Caliper, Electron Microscopy Sciences, Hatfield, PA, USA). The anterior portion of the whole, enucleated eye was glued into a custom fixture with the anterior chamber cannulated by a 30 gauge needle. Then, the eye was placed in a water bath at 20°C under a dissecting microscope (Carl Zeiss Microimaging, Thornwood, NY). The globe was oriented with the superior pole toward the camera, providing a view of the nasal-temporal sclera in the measuring plane. For scleral inflation, IOP was controlled through the cannula and measured with an in-line pressure transducer (Sensotech Inc, Wayne, NJ). Scleral displacement was measured during inflation using a two-dimensional (2D) digital image correlation (DIC)

system, which consisted of a CCD video camera (Grasshopper, model Gras-20S4M-C, Point Grey Research, Inc., Richmond, BC, Canada) attached to the dissecting microscope and a commercial DIC software package (Vic-2D, Correlated Solutions, Columbia, SC).

The eyes underwent two load-unload inflations from a reference pressure of 6–10 mm Hg (at which the sclera had no folds) to 30 mm Hg and back to reference pressure, then a third inflation to 30 mm Hg with pressure held at 30 mm Hg for 30 minutes, with a loading rate of 0.25 mm Hg/s for both load-unload and ramp-hold inflations (Nguyen et al., 2013). The analyses of scleral displacement presented here are from the loading portion of the first load-unload and from the ramp-hold to determine creep rate.

The strains in two directions, circumferential and meridional, were calculated for each eye from the DIC-determined position and displacement measurements, using the method described in detail in Nguyen et al. 2013 and briefly summarized here. For calculation of effective circumferential strain, we examined digital images of the nasal and temporal scleral edges from a superior view of the eye in the fixture. A series of points were marked manually every 0.1 mm along the scleral edge from the nerve head to the fixture along both the nasal and temporal sclera. DIC provided X-Y positions of selected points along both scleral edges at the reference pressure and the x-y positions after displacement ( $u_X$  and  $u_Y$ ) for each subsequent pressure. The deformed positions of the points were calculated as:  $x = X + u_X$  and  $y = Y + u_Y$ . The displacements and reference coordinates were used to calculate arc length coordinates,  $s$ , along the nasal and temporal scleral edge. Then, the effective circumferential strain was calculated from the change in the distance separating two points on the nasal and temporal scleral edge at the same  $s$ , which corresponded to a series of the nasal-temporal diameters at each  $s$  (see Nguyen et al., 2013). This would equal the circumferential strain for a pressurized spherical and spheroidal shell.

The meridional strains for the temporal and nasal edges of the sclera were calculated as the change in length of the scleral edges from  $s = 0.2$  mm to 1.5 mm from the ONH. To calculate the length of the scleral edge, a generalized ellipse was fit to the DIC-measured  $(X_k, Y_k)$  positions at the reference pressure and to the deformed  $(x_k, y_k)$  positions at each subsequent pressure, in order to smooth the DIC measurements (Figure 1). Corresponding points  $(X_k^e, Y_k^e)$  on the ellipse describing the undeformed scleral edge, and  $(x_k^e, y_k^e)$  on the ellipse describing the deformed scleral edge were calculated from the polar angle of the DIC positions from the major axis of the fitted ellipse. The length of the undeformed ( $L_\phi$ ) and deformed edge ( $l_\phi$ ) were calculated as:

$$\begin{aligned} L_\phi &= \sum_{k=1}^{15} \sqrt{(X_{k+1}^e - X_k^e)^2 + (Y_{k+1}^e - Y_k^e)^2}, \\ l_\phi &= \sum_{k=1}^{15} \sqrt{(x_{k+1}^e - x_k^e)^2 + (y_{k+1}^e - y_k^e)^2}, \end{aligned} \quad [1]$$

where  $k = 1..15$ , the number of the point along the ellipse.

The meridional strain in the region 0.2 mm–1.5 mm, was calculated separately for the nasal and for the temporal scleral edges as:

$$\text{meridional strain} = \frac{l_{\phi} - L_{\phi}}{L_{\phi}}, \quad [2]$$

To verify that the ellipse fit only reduced the variation associated with DIC noise and did not otherwise alter the measured pressure-strain response, the raw DIC position measurements were used to calculate the meridional strain for all control specimens at 26 mm Hg and 30 mm Hg and the results were compared to those using the smoothed positions. For both the nasal and temporal edges at both pressure levels, the difference in the raw and smoothed strains averaged over all specimens were less than  $\pm 0.001$ , which was smaller than the resolution of the DIC measurements.

Each specimen underwent two load—unload tests from reference IOP to 30 mm Hg and immediate return to reference, followed by a ramp—hold test, involving a loading to 30 mm Hg and holding at that pressure for 30 minutes with return to baseline to estimate creep rate. For the meridional creep rate analysis, the displacements were measured using DIC at 6 time points, one every 5 minutes, during the ramp—hold portion. Using the initial reference image from the first load-unload (used in the meridional analysis) the displacement was measured at each 5-minute time point to calculate the circumferential and meridional strains. Then, a linear regression was fit to these points for each eye and taken as the creep rates.

## 2.5. Scleral Thickness Measurements

Scleral thickness was measured on both fresh, unfixed sclera under a dissecting microscope and on histological sections embedded in epoxy, as described in a previous publication (Cone-Kimball et al., 2013). For fresh tissue thickness measurements, we used the inflation tested eyes (see section 4 in Methods). An eyepiece micrometer with the Zeiss dissecting microscope was used (Electron Microscopy Sciences, Hatfield, PA) to measure scleral specimens prepared with a razor blade to a resolution of  $\pm 0.01$  mm. Three strips, each 0.33 mm wide and 2.5 mm long, were cut from the superior sclera. Thickness measurements were made at 6 locations, every 0.5 mm, starting at the optic nerve head (ONH) and continuing anteriorly to the limbus.

For comparison to fresh measurements, fixed tissues were prepared in the following manner. Animals were euthanized and then perfused with 4% paraformaldehyde in 0.1 M phosphate buffer. The same eyes were also used for histological retinal analysis and optic nerve axon counts (see section 2.6 in Methods). After perfusion, eyes were enucleated and superior sclera was marked and the optic nerve was removed. The ONH was removed using a trephine and then it and the remaining sclera were fixed in 1% osmium tetroxide, dehydrated in ethanol, and stained with 1% uranyl acetate for 1 hour. Sclera was embedded in epoxy resin and 1 micron sections were stained with 1% toluidine blue. Images were taken using a 100x oil objective on a Zeiss light microscope (Carl Zeiss MicroImaging, Thornwood, NY) and a total of nine measurements were made for each animal and analyzed with Metamorph Image Analysis software (Molecular Devices, Downingtown, PA).

## 2.6. Histological Observations

For histological observations and for measurement of the outcome of glaucoma experiments to assess RGC axon loss, perfusion-fixed globes and optic nerves (N = 81 and N = 50, respectively) were post-fixed in 1% osmium tetroxide, epoxy-embedded, and sectioned at 1  $\mu\text{m}$  thickness. Digital images of optic nerve cross-sections were taken at low power to measure the total optic nerve area. Then, five,  $40 \times 40 \mu\text{m}$  fields (100x magnification, Cool Snap camera, Metamorph Image Analysis software; Molecular Devices, Downingtown, PA) were acquired, representing a random 9% sample of the total nerve area (Levkovitch-Verbin et al., 2002). A masked observer edited non-axonal elements from each image and the program calculated axon density. Average axon density/ $\text{mm}^2$  was multiplied by the individual nerve area to estimate axon number. Experimental eyes were compared to the mean axon number in pooled, fellow eye nerves of the appropriate strain and tissue fixation to yield percent axon loss.

In addition, from 1  $\mu\text{m}$  epoxy sections of retina, we quantitatively measured retinal layer thickness in GA-injected and in control eyes to evaluate possible damage either by GA injection treatment alone or by the glaucoma model (N=5). Thicknesses of the inner nuclear and outer nuclear layers were measured at 6 locations on each section by a masked observer.

## 2.7. Electroretinogram (ERG) Methods

ERG was recorded with an Espion instrument (Diagnosys LLC, Littleton, MA) as previously described (Oveson et al., 2011; Komeima et al., 2006; Komeima et al., 2007; Okoye et al., 2003; Ueno et al., 2008). Briefly, mice were kept in the dark overnight for dark adaptation. The mice were anesthetized with an intraperitoneal injection of ketamine hydrochloride (100 mg/kg body weight) and xylazine (5 mg/kg) body weight). Pupils were dilated with Midrin P containing 0.5% tropicamide and 0.5% phenylephrine, hydrochloride (Santen Pharmaceutical Co., Osaka, Japan), placed on a pad heated to 39°C, and platinum loop electrodes were placed on each cornea after application of gonioscopic prism solution (Alcon Labs, Fort Worth, TX). A reference electrode was inserted into the tail. The head of the mouse was held in a standardized position in a ganzfeld bowl illuminator that ensured equal illumination of the eyes. Recordings for both eyes were made simultaneously with balanced electrical impedance. Scotopic mean a-wave and b-wave amplitudes were calculated for 6 flashes of light at each of 11 light intensity levels. Then, photopic ERGs were recorded after light adapting the mice for 10 minutes. Photopic b-wave amplitudes were recorded using 3 flash intensities (4, 10, and 25  $\text{cd}\cdot\text{s}/\text{m}^2$ ) under a 25  $\text{cd}/\text{m}^2$  background light.

## 2.8. Fluorescence Recovery after Photobleaching (FRAP)

As a measure of scleral tissue diffusion for larger molecules, we employed FRAP, as recently published (Pease et al., 2014). In brief, freshly enucleated sclera was cleaned of extraocular tissue, separated from retina and choroid, and the optic nerve was removed flush with the sclera by a razor blade. We studied with the FRAP technique the sclera from 20 animals, 10 of which received only GA injections and 10 more that had GA injection and underwent experimental glaucoma. All scleral specimens were placed in 1 mg/ml fluorescein isothiocyanate-dextran (FITC-dextran) solution, molecular weight 40kDa

(FD-40, Sigma-Aldrich Corp, St. Louis, MO, USA) in phosphate buffer, incubated in the dark for 90 minutes, then mounted on slides in 25  $\mu$ L of FITC-dextran that were sealed with nail polish. Both the treated and untreated eyes (right) were studied from each group.

FRAP quantifies diffusion of fluorescently labeled molecules by measuring re-entry of unbleached dye into a region exposed to high intensity laser energy. Intensity of fluorescence re-entry over time is modeled as a bleach recovery function, whose half time was used as a measure of FITC-dextran diffusion. We used the Zeiss LSM510 NLO (Zeiss, Inc., New York, NY) with 488 nm laser at 2% power, a 488 main beam splitter and 415–735 band pass, and the Plan-Apochromat 63x/1.40 oil objective lens. The mean of 4–6 bleaches were analyzed with Zen 2010 LSM710 software, release 6.0 (Zeiss, Inc., New York, NY), fitting an exponential function to produce the primary outcome parameter, half time for recovery of baseline intensity after bleaching ( $t_{1/2}$ ).

## 2.9. Cross-Linking Assay

For the assay of advanced glycation end-products (AGE), a total of 38 CD1 animals were tested, including eyes with 3 GA injections (N=13), eyes with 3 buffer injections (N=15), bilateral control scleras (N=5), and scleras soaked in 0.5 M glyceraldehyde at room temperature for two hours (N=5). To include sufficient material for analysis, we pooled several scleral samples that had been treated similarly. Animals were anesthetized with intraperitoneal ketamine, xylazine, and acepromazine and their eyes were enucleated, with the sclera separated from the retina and choroid. Anterior and posterior sclera segments were separated. The posterior sclera included all the sclera within 2 mm of the optic nerve and the anterior sclera was the remaining sclera up to the limbus. Both were frozen and stored at  $-80^{\circ}\text{C}$ . Samples were manually macerated and sonicated for 15 seconds, then incubated in HEPES lysis buffer (100 mM HEPES pH 8.0, 200 mM 1 M KCl, 4 mM EDTA, 0.2% NP-40, 20% glycerol) with protease inhibitors (2 mM DTT, protease cocktail, 10 mM NaF, 5 nM okadaic acid, 5 nM calyculin A, 50 mM  $\beta$ -glycerolphosphate) on ice for one hour. Finally, samples were spun at  $4^{\circ}\text{C}$  at 15,000 g for 15 minutes. Supernatant was decanted and stored at  $-20^{\circ}\text{C}$  prior to testing.

Scleral protein concentrations in the extracted samples were determined by the Bradford assay (Bio-Rad, Hercules, CA). Quantification of AGE were determined using the OxiSelect Advanced Glycation End Product Competitive ELISA kit (Cellbiolabs, San Diego, CA), an assay measuring a variety of AGE. Briefly, in 96 well plates pre-adsorbed with an AGE conjugate, samples were introduced and AGE-specific primary antibody injected. Following incubation, the conjugated HRP secondary antibody was added. Sclera samples in triplicate were read at 450 nm using a SynergyMx microplate reader (Bio-Tek, Winooski, VT) and Gen5.1 software (Bio-Tek, Winooski, VT). The absorbance of scleral samples was compared to an AGE-BSA standard curve to yield AGE concentration in  $\mu\text{g/mL}$ .

## 2.10. Statistical Analysis

Outcomes were compared by t test for normally distributed parameters and Mann Whitney tests for parameters failing a normality test. Data from GA-injected eyes were compared to fellow eyes or to data from pooled, age-matched controls. Regression models were used to

estimate the effect of variables such as height and duration of IOP exposure on RGC axon loss when comparing results of experimental glaucoma trials.

### 3. Results

#### 3.1. Inflation Testing after GA Injection

Inflation testing consisted of two rapid load—unload tests to 30 mm Hg, followed by a load to 30 mm Hg held for 30 minutes. The pressure—strain in the first load—unload test was compared in eyes once, twice, or 3 times injected subconjunctivally with GA and in untreated control eyes (Figure 2; n = 12 (3X GA), n = 18 (2X GA), n = 12 (1X GA), and n = 28 (control)). The 3X GA injected eyes had significantly stiffer pressure—strain behavior than controls in both meridional and circumferential directions (Table 1). For example, the meridional strain at 30 mm Hg was significantly lower in GA injected eyes than controls ( $p = 0.002$ , t test), as was the mean circumferential strain for the entire sclera at 30 mm Hg ( $p = 0.05$ , t-test). Comparing the slopes of the meridional strains at 6 pressures during the load—unload test between reference IOP and 30 mm Hg, the 3X GA injected curve was significantly stiffer than the control values ( $p = 0.004$ ; best fit regression for 3X GA:  $y = 189644x^2 - 1251x + 11.9$ ,  $r^2 = 0.98$ , and for control:  $y = 28470x^2 - 152x + 10.5$ ,  $r^2 = 0.98$ ; Figure 2). Similarly, the creep rate during a 30 minute ramp—hold experiment was significantly lower after 3 GA injections than in control CD1 eyes. For example, in the circumferential direction, the mean creep rate in 4 sampled regions from the ONH to the anterior sclera ranged from 23 to 40% less after GA exposure than in controls ( $p = 0.055$  to  $0.009$ , t tests).

#### 3.2. Advanced Glycation End Product Assay (AGE)

The AGE concentration was 13.7  $\mu\text{g}/\text{mL}$  in the 3x GA injected sclera compared to 9.9  $\mu\text{g}/\text{mL}$  in the bilateral control group (data from combined posterior and anterior sclera), a  $37\% \pm 3.7\%$  (standard deviation) higher concentration of AGE with GA exposure than in controls ( $p < 0.003$ , t test, n = 13 GA-treated scleras and 15 controls). There was no consistent difference between posterior and anterior sclera in either controls or treated eyes.

#### 3.3. Effect of GA Injections on ERG, Retinal Histology, Scleral Thickness, and FRAP Diffusion

**3.3.1**—Scotopic ERG testing was performed after overnight dark adaptation, followed by photopic testing. There were no significant differences in a-wave and b-wave amplitudes between 3x GA injected and control eyes at 11 scotopic flash intensities and 3 photopic flash intensities (all  $p > 0.2$ , Figure 3). ERG values were similar to those previously published by Campochiaro et al. for mice (Miki et al., 2010).

**3.3.2**—Retinal histology was compared in 3X GA injected and control, uninjected mice in 1 micron, epoxy-embedded sections (n = 5 per group). GA-injected eyes had no apparent differences from normal in the appearance of RGC layer, nerve fiber layer, inner nuclear layer, outer nuclear layer or photoreceptor layer. The measured thicknesses of the inner and outer nuclear layers were not significantly different between GA and controls (Table 3).

**3.3.3. Scleral thickness measurements**—The average fresh, unfixated scleral thickness from ONH to limbus was 8.7% less for 3x GA injected sclera than that of age-matched, fellow eye controls ( $p = 0.2$  or greater for each of 6 regions). After tissue fixation, measurements in histological sections showed that the peripapillary scleral thickness had a complex structure. At approximately 200  $\mu\text{m}$  from the ONH, the sclera divides into two portions, one that adjoins the ONH and the other which courses posteriorly to join the dura mater surrounding the nerve (Figure 4). We therefore measured both the outer sclera prior to this division and the inner portion adjacent to the canal. Control CD1 outer scleral thickness (Table 4) was similar to our previously published peripapillary scleral thickness in CD1 mice ( $32.7 \pm 4.4 \mu\text{m}$ ) (Nguyen et al., 2013). After bead-induced glaucoma, both GA and non-GA injected eyes had significantly thicker outer sclera than controls ( $p = 0.02$  and  $0.0015$ ,  $t$  tests compared to matched controls; Table 4). The GA injection alone group was not significantly thicker than controls.

The mean inner peripapillary sclera thickness, immediately on either side of the nerve canal, was thicker across all groups than the outer peripapillary portion ( $p = 0.007$ ,  $t$ -test; Table 4). This inner peripapillary scleral thickness was not significantly different between GA injected (without glaucoma) and controls, but both glaucoma groups (with and without GA injection) had significantly thicker inner sclera than control (18% and 24% increase, respectively;  $p = 0.012$ ,  $0.017$ ,  $t$  test, 5 animals per group, Table 4). In both the outer and inner peripapillary sclera, the increase in thickness after glaucoma exposure was less in the GA injected than the non-injected eyes, but this difference did not reach significance ( $p = 0.4$ ).

**3.3.4**—Fluorescence recovery after photobleaching (FRAP) measurement yields a half time to recovery of original fluorescence ( $t_{1/2}$ ) that indicates poorer permeability of the sclera. In control sclera, we confirmed our prior finding (Pease et al., 2014) that the peripapillary sclera (outer) has the lowest permeability (Table 5) and that permeability is greater at 0.75 mm or 1.5 mm more anteriorly (toward the cornea; paired  $t$  tests:  $p < 0.0001$  and  $0.0009$ ; Table 5). Treatment with 3 GA injections (without experimental glaucoma) significantly decreased scleral permeability compared to controls in all 3 scleral zones ( $p = 0.001$ ). There was no significant difference between sclera treated with GA and sclera from eyes that underwent experimental glaucoma after GA treatment ( $p = 0.7$ ,  $t$  test). In our prior work, sclera from eyes that underwent experimental glaucoma also had lower permeability than fellow eye, control sclera (Pease et al., 2014).

### 3.4. Experimental Glaucoma: Effect of GA Injection

**3.4.1. First glaucoma experiment**—Unilateral, bead-induced glaucoma was produced in 42 mice one week after 3 GA injections over one week and in 46 mice that had 3 similarly timed buffer injections (final axon loss data was collected in 40 GA and 41 buffer eyes). Axial length and width increased with chronically elevated IOP in both 3x GA and 3x buffer injected eyes, with somewhat less elongation in GA eyes than in buffer eyes ( $p = 0.05$  for length difference,  $0.2$  for width difference,  $t$  test; Table 6). As might be expected, greater IOP exposure was associated with significantly greater RGC axon loss ( $p = 0.02$ , regression coefficient =  $0.0006$ , 95% C.I.:  $0.00007$ ,  $0.001$ , see Figure 5). Since there was a small, but

not significantly higher IOP exposure in the buffer compared to the GA group (197 vs 169 mm Hg—days, positive IOP integral,  $p = 0.4$ ,  $t$  test), we compared the groups taking IOP exposure into account in regression models.

Compared to fellow eye controls, RGC axon loss was greater in the 3x GA-injected group than buffer-injected controls. In a regression model comparing RGC axon loss between treatment groups including IOP exposure, the RGC axon loss was significantly greater in the GA group compared to buffer group (regression model  $p = 0.01$ ; regression coefficient (treatment GA vs control) = 0.1275 (SE = 0.07953; 95% CI = -0.03114 to 0.2861; coefficient (positive integral) = 0.0005922 (SE = 0.0002609; 95% CI = 0.00007174 to 0.001113). The distribution of RGC axon loss in GA compared to buffer injected eyes was particularly evident in the axon loss range between 10–60% when each animal was ranked by degree of injury (Figure 6). The median axon loss was 62% in GA compared to 34% loss in the buffer-injected group (mean  $\pm$  standard deviation for GA:  $53 \pm 34\%$  loss, buffer:  $41 \pm 37\%$  loss,  $n = 40$  and  $41$  mice).

**3.4.2. Second glaucoma experiment**—We compared RGC axon loss with bead induced glaucoma between 3x GA injected eyes and control, uninjected eyes, again with glaucoma induction one week after the GA injections. With 20 mice in each group, GA injected eyes experienced nearly twice the RGC axon loss of the controls, a mean of  $44.6 \pm 32.4\%$  RGC axon loss for GA group compared to  $23.0 \pm 30.9\%$  loss for the uninjected controls (Table 7). There was only a slight difference in IOP exposure between the GA and controls. Multivariable regression analysis including cumulative IOP exposure as an independent variable showed that there was significantly greater loss in GA injected eyes compared to controls ( $p = 0.049$ , regression coefficient (treatment GA vs control) = -0.2228 (SE = 0.1087; 95% CI = -0.4444 to -0.001261; for positive integral IOP term in this regression model, regression coefficient = 0.0001981 (SE = 0.0002535; 95% CI = -0.0003184 to 0.0007146).

To test for a detrimental effect of GA injection alone on RGC axon number, we counted axon number in 10 mouse nerves 6 weeks after 3 GA injections. The total RGC axon counts of 3x GA injected eyes were not significantly different from control CD1 mice, indicating that the greater loss of RGC in the GA group in the glaucoma experiments was not due to a primary toxic effect of GA alone.

## 4. Discussion

We show for the first time, to our knowledge, that experimental alteration of scleral composition can affect the rate of RGC damage in a mouse glaucoma model. GA treatment of the sclera was associated with greater RGC axon loss than among control eyes in 2 experiments. While the mouse model leads to a difference among animals exposed to elevated pressure in the degree of axon loss, the distribution and the mean axon loss were significantly different in the GA treated mice exposed to glaucoma compared to either control or buffer treated animals. GA treatment increased scleral cross-linking, decreased scleral permeability, and increased scleral stiffness. GA exposure alone did not produce

RGC axon loss through a direct toxic effect, nor was there any damage to other retinal layers as measured by histological evaluation or ERG.

Our data suggest that the alterations in the sclera induced by GA treatment led to greater RGC axon loss due to decreased scleral strain (increased stiffness), especially in the peripapillary region. In monkey (Girard et al., 2009; Downs et al., 2005) and human eyes (Coudrillier et al., 2012), the peripapillary sclera exhibits the greatest strain from IOP, compared to more anterior regions of the sclera, and its connective tissue elements are specifically organized in a circumferential manner to resist this strain. Modeling studies point to the importance of peripapillary scleral strain on the ONH and to an interaction between ONH features and those of the surrounding sclera (Sigal et al., 2011a; Sigal et al., 2005; Normal et al., 2011). It can be predicted that if the scleral peripapillary ring enlarges with an increase in IOP, the width of the ONH would increase, potentially causing effects such as anterior movement of the ONH, as is actually observed in early experimental glaucoma in young monkeys (Downs et al., 2005; Yang et al., 2011; Coudrillier, 2013). On the other hand, if the peripapillary sclera were relatively more rigid (such as after GA treatment), the LC might be more likely to bow outward with an IOP increase (Sigal et al., 2011b). Either widening of the scleral canal (with a more elastic peripapillary sclera) or backward bowing of the lamina cribrosa (with a more rigid sclera) could be protective or detrimental to RGC axons passing through the ONH (Quigley and Cone, 2013; Strouthidis and Girard, 2013). While modeling points to important factors for study, experimental alteration of parameters under controlled conditions can directly test the effects of each component. Thornton et al. (2009) produced stiffening of excised pig eyes in peripapillary sclera and speculated that this might be beneficial in glaucoma. Our data suggest that experimental stiffening of the sclera has a statistically significant association with greater, not less RGC damage, at least in CD1 mice.

There are important similarities and differences in the anatomy of the mouse and human peripapillary sclera and ONH. While the mouse ONH has no connective tissue, its astrocytes mimic the configuration of the connective tissue LC of monkeys and humans (Sun et al., 2009). The ONH and globe diameter of the mouse are proportionately 10 times smaller than those in the human eye and mouse scleral thickness in mouse is about 1/10<sup>th</sup> that of the human eye. The mouse sclera shares important features of human sclera, such as the ring of circumferentially oriented collagen and elastin in the peripapillary sclera (Cone-Kimball, 2013). Likewise, with experimental glaucoma, the mouse ONH widens posterior to Bruch's membrane (Cone-Kimball, et al., 2013), as does the human eye (Quigley et al., 1983). With experimental IOP elevation, the mouse RGC axons develop acute abnormalities at the ONH at the level of the sclera (Howell et al., 2007), as do humans (Quigley et al., 1981). The relevance of mouse and rat experimental glaucoma to human disease is further supported by the fact that only RGC die with moderate IOP elevations, as in humans (Kielczewski et al., 2005). We presume that the effect of GA in the mouse eye was on the sclera, not the lamina cribrosa, since the mouse has minimal if any connective tissues within the ONH.

Since an increase in scleral cross-linking led to worse glaucoma damage, it would be logical to test whether weakening of scleral connective tissue components would be beneficial. Enzymatic digestion of *post mortem* human ONH alters its biomechanical properties (Spoerl

et al., 2005), and digestion with chondroitinase alters scleral strain in porcine globes in the opposite direction to that seen with GA treatment (Murienne et al., 2013). Investigations of experimental glaucoma both in monkeys (Burgoyne et al., 2005) and mice (Cone et al., 2010) suggest that both baseline scleral structure and its dynamic response to elevated IOP may be important determinants of glaucomatous damage. Therapeutically beneficial approaches may necessitate more than baseline alterations of fiber or matrix components of sclera. Mice with a mutation in collagen 8 $\alpha$ 2 (Aca23) are protected against injury in experimental murine glaucoma (Steinhart et al., 2012). Aca23 mice have stiffer sclera at baseline, as do our GA treated CD1 mice in the present experiment, yet the resultant RGC axon loss differed in the 2 groups. The sclera is stiffer by inflation testing (Coudrillier et al., 2012) and indirect evaluation (Hommer et al., 2008) in human glaucoma eyes and in the sclera of experimental glaucoma mice of 3 strains (Nguyen et al., 2013). It is not yet established whether the greater stiffness of human glaucoma eyes is present at baseline, whether it develops as a response to the disease, or both. Recent detailed studies in mouse glaucoma found a decrease in non-fibrillar scleral components, increased thickness and number of fibrillar lamellae, and a shift toward lamellae oriented antero-posteriorly--all consistent with the increased measured stiffness (Cone-Kimball et al., 2013). Experimental glaucoma induces alterations in the mouse sclera that include increased fibroblast division, transition to a myofibroblast phenotype, and activation of proteins involved in integrin-linked signaling and actin cytoskeletal pathways (Oglesby et al., unpublished data). This suggests that the scleral response to elevated IOP may be as important as its baseline state in determining sensitivity to damage. There have been attempts to include a dynamic scleral remodeling process after experimental IOP increase in models describing the eye's response to glaucoma (Grytz et al., 2012). However, more information is needed on the details of this dynamic response before the models can be considered indicative of the true behavior.

One component of the dynamic scleral response to experimental glaucoma is upregulation of TGF $\beta$  signaling, which was identified in proteomic analysis of mouse glaucoma sclera (Oglesby et al., 2014). This pathway has previously been involved in both trabecular meshwork (Prendes et al., 2013) and ONH responses in glaucoma (Lukas et al. 2008; Fuchshofer and Tamm, 2012). Human scleral anatomy and physiology change with age, and are affected by diseases such as myopia (Rada et al., 2006; McBrien et al., 2006; Wiesel et al., 1977) and glaucoma (Pijanka et al., 2012; Norman et al., 2010). Scleral stiffness increases with age (Coudrillier et al., 2012) and the complement of connective tissue in the LC is denser in the elderly compared to younger eyes (Coudrillier et al., 2012; Quigley, 1977). TGF $\beta$  inhibition of mouse models of Marfan syndrome (Habashi et al., 2013) and humans affected by the Marfan syndrome (Lacro et al., 2013) yielded beneficial effects. Appropriate modification of important scleral processes in glaucoma could represent important new therapeutic opportunities.

The present experiments have certain limitations. As discussed, mouse eyes and the ocular and systemic responses in the mouse glaucoma model should be interpreted with caution in respect to human glaucoma. CD1 mice have the advantage that they undergo significant and selective loss of RGC with experimental IOP elevation. They are an outbred group of mice, so therapy trials in this group are more generalizable than in inbred mice. We have demonstrated that a specific alteration in scleral tissues was associated with an increase in

RGC axon loss. We have attempted to assess off-target effects of GA injection that could explain these results. The glaucoma experiment was repeated to confirm the association. However, we cannot yet rule out the possibility that the detrimental effect of GA acted through a mechanism other than scleral alteration. While we found that GA treatment increased scleral cross-linking, it also decreased scleral permeability. This may point to an effect of GA treatment on non-fibrillar components of the sclera as contributing elements in protecting RGC from injury.

In summary, GA-treated mouse eyes had greater RGC axon loss from elevated IOP than either buffer-injected or control eyes, controlling for level of IOP exposure. GA exposure alone did not affect RGC number, retinal structure or function, though it increased scleral crosslinking, decreased scleral permeability, and produced a steeper pressure—strain behavior. To our knowledge, this represents the first experimental alteration of the sclera that alters susceptibility to RGC damage. Further study of the dynamic responses of the sclera to glaucoma may present therapeutic approaches that could be additive to IOP-lowering.

## Acknowledgments

This work was supported in part by PHS research grants EY 02120 and EY 01765 (Dr Quigley, and Wilmer Institute Core grant), EY021500 and support from the BrightFocus Foundation (Dr. Nguyen) and by unrestricted support from Saranne and Livingston Kosberg and from William T. Forrester. The funders had no role in study design, data collection and analysis, decision to publish, or preparation of the manuscript.

The authors would like to thank Peter Campochiaro for his expertise in assisting with electroretinography.

## References

- Avetisov ES, Savitskaya NF, Vinetskaya MI, Iomdina EN. A study of biochemical and biomechanical qualities of normal and myopic eye sclera in humans of different age groups. *Metab Pediatr Syst Ophthalmol*. 1984; 7:183–188. [PubMed: 6678372]
- Backhouse S, Phillips JR. Effect of induced myopia on scleral myofibroblasts and in vivo ocular biomechanical compliance in the guinea pig. *Invest Ophthalmol Vis Sci*. 2010; 51:6162–6171. [PubMed: 20592231]
- Bengtsson B, Heijl A. Diurnal IOP fluctuation: not an independent risk factor for glaucomatous visual field loss in high-risk ocular hypertension. *Graefe's Arch Clin Exper Ophthalmol*. 2005; 243:513–8. [PubMed: 15756577]
- Boland MV, Quigley HA. Risk factors and open-angle glaucoma: concepts and applications. *J Glaucoma*. 2007; 16:406–418. [PubMed: 17571004]
- Burgoyne CF, Downs JC, Bellezza AJ, Suh J-KF, Hart RT. The optic nerve head as a biomechanical structure: a new paradigm for understanding the role of IOP-related stress and strain in the pathophysiology of glaucomatous optic nerve head damage. *Prog Ret Eye Res*. 2005; 24:39–73.
- Cone FE, Gelman SE, Son JL, Pease ME, Quigley HA. Differential susceptibility to experimental glaucoma among 3 mouse strains using bead and viscoelastic injection. *Exp Eye Res*. 2010; 91:415–24. [PubMed: 20599961]
- Cone-Kimball E, Nguyen C, Oglesby EN, Pease ME, Steinhart MR, Quigley HA. Scleral structural alterations associated with chronic experimental intraocular pressure elevation in mice. *Mol Vis*. 2013; 19:2023–39. [PubMed: 24146537]
- Congdon NG, Broman AT, Bandeen-Roche K, Grover D, Quigley HA. Central corneal thickness and corneal hysteresis associated with glaucoma damage. *Am J Ophthalmol*. 2006; 141:868–75. [PubMed: 16527231]

- Coudrillier B, Tian J, Alexander S, Myers KM, Quigley HA, Nguyen TD. Biomechanics of the human posterior sclera: age- and glaucoma-related changes measured using inflation testing. *Invest Ophthalmol Vis Sci.* 2012; 53:1714–28. [PubMed: 22395883]
- Curtin B. Physiopathologic aspects of scleral stress-strain. *Trans Am Ophthalmol Soc.* 1969; 67:417–461. [PubMed: 5381306]
- Danilov NA, Yu N, Ignatieva N, Iomdina EN, Semenova SA, Rudenskaya GM, Grokhovskaya TE, Lunin VV. Stabilization of scleral collagen by glycerol aldehyde cross-linking. *Biochim Biophys Acta.* 2008; 1780:764–772.
- Downs JC, Suh J-KF, Thomas KA, Belleza AJ, Hart RT, Burgoyne CF. Viscoelastic material properties of the peripapillary sclera in normal and early-glaucoma monkey eyes. *Invest Ophthalmol Vis Sci.* 2005; 46:540–546. [PubMed: 15671280]
- Fazio MA, Grytz R, Morris JS, Bruno L, Gardiner SK, Girkin CA, Downs JC. Age-related changes in human peripapillary scleral strain. *Biomech Model Mechanobiol.* 2013 [Epub ahead of print].
- Friberg TR, Lace JW. A comparison of the elastic properties of human choroid and sclera. *Exp Eye Res.* 1988; 47:429–436. [PubMed: 3181326]
- Fuchshofer R, Tamm ER. The role of TGF- $\beta$  in the pathogenesis of primary open-angle glaucoma. *Cell Tissue Res.* 2012; 347:279–290.
- Gaasterland D, Kupfer C. Experimental glaucoma in the rhesus monkey. *Invest Ophthalmol Vis Sci.* 1974; 13:455–7.
- Gelman S, Cone FE, Pease ME, Nguyen TD, Myers K, Quigley HA. The presence and distribution of elastin in the posterior and retrobulbar regions of the mouse eye. *Exp Eye Res.* 2010; 90:210–215. [PubMed: 19853602]
- Geraghty B, Jones SW, Rama P, Akhtar R, Elsheikh A. Age-related variations in the biomechanical properties of human sclera. *J Mech Behav Biomed Mater.* 2012; 16:181–191. [PubMed: 23182387]
- Girard MJA, Downs JC, Burgoyne CF, Suh JK. Experimental surface strain mapping of porcine peripapillary sclera due to elevations of intraocular pressure. *J Biomech Eng.* 2008; 130:041017. [PubMed: 18601459]
- Girard MJA, Suh JK, Bottlang M, Burgoyne CF, Downs JC. Scleral biomechanics in aging monkey eye. *Invest Ophthalmol Vis Sci.* 2009; 50:5226–5237. [PubMed: 19494203]
- Greene PR, McMahon TA. Scleral creep versus temperature and pressure *in vitro*. *Exp Eye Res.* 1979; 29:527–537. [PubMed: 527689]
- Grytz R, Girkin CA, Libertaux V, Downs JC. Perspectives on biomechanical growth and remodeling mechanisms in glaucoma. *Mech Res Commun.* 2012; 42:92–106.
- Habashi JP, Doyle JJ, Holm TM, Aziz H, Schoenhoff F, Bedja D, Chen Y, Modiri AN, Judge DP, Dietz HC. Angiotensin II type 2 receptor signaling attenuates aortic aneurysm in mice through ERK antagonism. *Science.* 2011; 332:361–5. [PubMed: 21493863]
- Heijl A, Leske MC, Bengtsson B, Hyman L, Bengtsson B, Hussein M. The Early Manifest Glaucoma Trial Group. Reduction of intraocular pressure and glaucoma progression. *Arch Ophthalmol.* 2002; 120:1268–79. [PubMed: 12365904]
- Hommer A, Fuchsjäger-Mayrl G, Resch H, Vass C, Garhofer G, Schmetterer L. Estimation of ocular rigidity based on measurements of pulse amplitude using pneumotonometry and fundus pulse using laser interferometry in glaucoma. *Invest Ophthalmol Vis Sci.* 2008; 49:4046–4050. [PubMed: 18487379]
- Howell GR, Libby RT, Jakobs TC, Smith RS, Phalan FC, Barter JW, Barbay JM, Marchant JK, Mahesh N, Porciatti V, Whitmore AV, Masland RH, John SW. Axons of retinal ganglion cells are insulted in the optic nerve early in DBA/2J glaucoma. *J Cell Biol.* 2007; 179:1523–37. [PubMed: 18158332]
- Ihanamaki T, Salminen H, Säämänen AM, Pelliniemi LJ, Hartmann DJ, Sandberg-Lall M, Vuorio E. Age-dependent changes in the expression of matrix components in the mouse. *Exp Eye Res.* 2001; 72:423–431. [PubMed: 11273670]
- Keeley F, Morin J, Vesely S. Characterization of collagen from normal human sclera. *Exp Eye Res.* 1984; 39:533–542. [PubMed: 6519194]

- Kielczewski JL, Pease ME, Quigley HA. The effect of experimental glaucoma and optic nerve transection on amacrine cells in the rat retina. *Invest Ophthalmol Vis Sci.* 2005; 46:3188–96. [PubMed: 16123418]
- Komeima K, Rogers BS, Lu L, Campochiaro PA. Antioxidants reduce cone cell death in a model of retinitis pigmentosa. *Proc Natl Acad Sci USA.* 2006; 103:11300–11305. [PubMed: 16849425]
- Komeima K, Rogers BS, Campochiaro PA. Antioxidants slow photoreceptor cell death in mouse models of retinitis pigmentosa. *J Cell Physiol.* 2007; 213:809–815. [PubMed: 17520694]
- Lacro RV, Guey LT, Dietz HC, Pearson GD, Yetman AT, Gelb BD, Loeys BL, Benson DW, Bradley TJ, De Backer J, Forbus GA, Klein GL, Lai WW, Levine JC, Lewin MB, Markham LW, Paridon SM, Pierpont ME, Radojewski E, Selamet Tierney ES, Sharkey AM, Wechsler SB, Mahony L. Characteristics of children and young adults with Marfan syndrome and aortic root dilation in a randomized trial comparing atenolol and losartan therapy. *Am Heart J.* 2013; 165:828–835. [PubMed: 23622922]
- Levkovitch-Verbin H, Quigley HA, Martin KR, Valenta D, Baumrind LA, Pease ME. Translimbal laser photocoagulation to the trabecular meshwork as a model of glaucoma in rats. *Invest Ophthalmol Vis Sci.* 2002; 43:402–410. [PubMed: 11818384]
- Lukas TJ, Miao H, Chen L, Riordan SM, Li W, Crabb AM, Wise A, Du P, Lin SM, Hernandez MR. Susceptibility to glaucoma: differential comparison of the astrocyte transcriptome from glaucomatous African American and Caucasian American donors. *Genome Biol.* 2008; 9:R111. [PubMed: 18613964]
- Malik NS, Moss SJ, Ahmed N, Furth AJ, Wall RS, Meek KM. Ageing of the human corneal stroma: structural and biochemical changes. *Biochimica Biophysica Acta.* 1992; 1138:222–228.
- Mattson MS, Huynh J, Wiseman ME, Coassin M, Kornfield JA, Schwartz D. An in vitro intact globe expansion method for evaluation of cross-linking treatments. *Invest Ophthalmol Vis Sci.* 2010; 51:3120–3128. [PubMed: 20071684]
- McBrien NA, Lawlor P, Gentle A. Scleral remodeling during the development of and recovery from axial myopia in the tree shrew. *Invest Ophthalmol Vis Sci.* 2000; 41:3713–3719. [PubMed: 11053267]
- McBrien NA, Cornell LM, Gentle A. Structural and ultrastructural changes to the sclera in a mammalian model of high myopia. *Invest Ophthalmol Vis Sci.* 2001; 42:2179–2187. [PubMed: 11527928]
- Miki A, Miki K, Ueno S, Wersinger DM, Berlinicke C, Shaw GC, Usui S, Wang Y, Zack DJ, Campochiaro PA. Prolonged blockade of VEGF receptors does not damage retinal photoreceptors or ganglion cells. *J Cell Physiol.* 2010; 224:262–72. [PubMed: 20232317]
- Morrison JC, Dorman-Pease ME, Dunkelberger GR, Quigley HA. Optic nerve head extracellular matrix in primary optic atrophy and experimental glaucoma. *Arch Ophthalmol.* 1990; 108:1020–4. [PubMed: 2369339]
- Morrison JC, Moore CG, Deppmeier LM, Gold BG, Meshul CK, Johnson EC. A rat model of chronic pressure-induced optic nerve damage. *Exp Eye Res.* 1997; 64:85–96. [PubMed: 9093024]
- Morrison JC, Nylander KB, Lauer AK, Cepurna WO, Johnson E. Glaucoma drops control intraocular pressure and protect optic nerves in a rat model of glaucoma. *Invest Ophthalmol Vis Sci.* 1998; 39:526–31. [PubMed: 9501862]
- Murienne, BJ.; Quigley, HA.; Nguyen, T. The role of glycosaminoglycans in the mechanical behavior of the posterior sclera. *ARVO; Ft. Lauderdale, FL, 52-A0039:* 2013.
- Myers KM, Cone FE, Quigley HA, Gelman SE, Pease ME, Nguyen TD. The *in vitro* inflation response of mouse sclera. *Exp Eye Res.* 2010; 91:866–875. [PubMed: 20868685]
- Nguyen C, Cone FE, Nguyen TD, Coudrillier B, Pease ME, Steinhart MR, Oglesby EN, Quigley HA. Studies of scleral biomechanical behavior related to susceptibility for retinal ganglion cell loss in experimental mouse glaucoma. *Invest Ophthalmol Vis Sci.* 2013; 54:1767–80. [PubMed: 23404116]
- Norman RE, Flanagan JG, Rausch SMK, Sigal IA, Tertinegg I, Eilaghi A, Portnoy S, Sled JG, Ethier CR. Dimensions of the human sclera: Thickness measurement and regional changes with axial length. *Exp Eye Res.* 2010; 90:277–284. [PubMed: 19900442]

- Normal RE, Flanagan JG, Sigal IA, Rausch SMK, Tertinegg I, Ethier CR. Finite element modeling of the human sclera: Influence on optic nerve head biomechanics and connections with glaucoma. *Exp Eye Res.* 2011; 93:4–12. [PubMed: 20883693]
- Nouri-Mahdavi K, Hoffman D, Coleman A, Liu G, Li G, Gaasterland D, Caprioli J. Predictive factors for glaucomatous visual field progression in the Advanced Glaucoma Intervention Study. *Ophthalmology.* 2004; 111:1627–35. [PubMed: 15350314]
- Oglesby E, Tezel G, Cone-Kimball E, Steinhart M, Jeffreys J, Pease M, Quigley H. Sclera fibroblast response to experimental glaucoma in mice. *Invest Ophthalmol Vis Sci.* [Unpublished results].
- Okoye G, Zimmer J, Sung J, Gehlbach P, Deering T, Nambu N, Hackett SF, Melia M, Esumi N, Zack DJ, Campochiaro PA. Increased expression of BDNF preserves retinal function and slows cell death from rhodopsin mutation or oxidative damage. *J Neurosci.* 2003; 23:4164–4172.
- Oveson BC, Iwase T, Hackett SF, Lee SY, Usui S, Sedlak TW, Snyder SH, Campochiaro PA, Sung JU. Constituents of bile, bilirubin and TUDCA, protect against oxidative stress-induced retinal degeneration. *J Neurochem.* 2011; 116:144–53. [PubMed: 21054389]
- Pease ME, Hammond J, Quigley HA. Manometric calibration and comparison of TonoLab and TonoPen tonometers in rats with experimental glaucoma and in normal mice. *J Glaucoma.* 2006; 15:512–9. [PubMed: 17106364]
- Pease ME, Cone FE, Gelman SE, Son JL, Quigley HA. Calibration of the TonoLab tonometer in mice with spontaneous or experimental glaucoma. *Invest Ophthalmol Vis Sci.* 2011; 52:858–864. [PubMed: 20720229]
- Pease ME, Oglesby EN, Cone-Kimball E, Jeffreys JL, Steinhart MR, Kim AJ, Hanes J, Quigley HA. Scleral permeability varies by mouse strain and is decreased by chronic experimental glaucoma. *Invest Ophthalmol Vis Sci.* 2014 Feb 20. [Epub ahead of print].
- Pijanka JK, Coudrillier B, Ziegler K, Sorensen T, Meek KM, Nguyen TD, Quigley HA, Boote C. Quantitative mapping of collagen fiber orientation in non-glaucoma and glaucoma posterior human sclerae. *Invest Ophthalmol Vis Sci.* 2012; 53:5258–5270. [PubMed: 22786908]
- Prendes MA, Harris A, Wiostko BM, Gerber AL, Siesky B. The role of transforming growth factor  $\beta$  in glaucoma and the therapeutic implications. *Br J Ophthalmol.* 2013; 97:680–686. [PubMed: 23322881]
- Quigley HA. The pathogenesis of reversible cupping in congenital glaucoma. *Am J Ophthalmol.* 1977; 84:358–370. [PubMed: 900230]
- Quigley HA, Green WR. The histology of human glaucoma cupping and optic nerve damage: clinicopathologic correlation in 21 eyes. *Ophthalmology.* 1979; 10:1803–27. [PubMed: 553256]
- Quigley HA, Addicks EM, Green WR, Maumenee AE. Optic nerve damage in human glaucoma. II. The site of injury and susceptibility to damage. *Arch Ophthalmol.* 1981; 99:635–49. [PubMed: 6164357]
- Quigley HA, Hohman RM, Addicks EM, Massof RS, Green WR. Morphologic changes in the lamina cribrosa correlated with neural loss in open-angle glaucoma. *Am J Ophthalmol.* 1983; 95:673–91. [PubMed: 6846459]
- Quigley HA, Broman A. The number of persons with glaucoma worldwide in 2010 and 2020. *Br J Ophthalmol.* 2006; 90:151–156.
- Quigley HA, Cone FE. Development of diagnostic and treatment strategies for glaucoma through understanding and modification of scleral and lamina cribrosa connective tissue. *Cell Tissue Res.* 2013; 353:231–44. [PubMed: 23535950]
- Rada JA, Achen VR, Penugonda S, Schmidt RW, Mount BA. Proteoglycan composition in the human sclera during growth and aging. *Invest Ophthalmol Vis Sci.* 2000; 41:1639–1648. [PubMed: 10845580]
- Rada JAS, Shelton S, Norton TT. The sclera and myopia. *Exp Eye Res.* 2006; 82:185–200. [PubMed: 16202407]
- Sigal IA, Flanagan JG, Ethier CR. Factors influencing optic nerve head biomechanics. *Invest Ophthalmol Vis Sci.* 2005; 46:4189–99. [PubMed: 16249498]
- Sigal IA, Yang H, Roberts MD, Burgoyne CF, Downs JC. IOP-induced lamina cribrosa displacement and scleral canal expansion: an analysis of factor interactions using parameterized eye-specific models. *Invest Ophthalmol Vis Sci.* 2011a; 52:1896–907. [PubMed: 20881292]

- Sigal IA, Yang H, Roberts MD, Grimm JL, Burgoyne CF, Demirel S, Downs JC. IOP-induced lamina cribrosa deformation and scleral canal expansion: Independent or related? *Invest Ophthalmol Vis Sci.* 2011b; 52:9023–9032. [PubMed: 21989723]
- Spoerl E, Boehm AG, Pillunat LE. The influence of various substances on the biomechanical behavior of lamina cribrosa and peripapillary sclera. *Invest Ophthalmol Vis Sci.* 2005; 46:1286–90. [PubMed: 15790892]
- Steinhart MR, Cone FE, Nguyen C, Nguyen TD, Pease ME, Puk O, Graw J, Oglesby E, Quigley HA. Mice with an induced mutation in Collagen 8A2 develop larger eyes and are resistant to retinal ganglion cell damage in an experimental glaucoma model. *Mol Vis.* 2012; 18:1093–1106. [PubMed: 22701298]
- Strouthidis NG, Girard MJA. Altering the way the optic nerve head responds to intraocular pressure—a potential approach to glaucoma therapy. *Curr Opin Pharmacol.* 2013; 13:83–89. [PubMed: 22999652]
- Sun D, Lye-Barthel M, Masland RH, Jakobs TC. The morphology and spatial arrangement of astrocytes in the optic nerve head of the mouse. *J Comp Neurol.* 2009; 516:1–19. [PubMed: 19562764]
- Tejedor J, de la Villa P. Refractive changes induced by form deprivation in the mouse eye. *Invest Ophthalmol Vis Sci.* 2003; 44:32–36. [PubMed: 12506052]
- Terai N, Schlotzer-Schrehardt E, Spoerl E, Hornykewycz K, Haentzschel J, Haustein M, Pillunat L. Biomechanical and morphological differences between the scleral canal ring and a peripheral sclera ring in the porcine eye. *Ophthalmic Res.* 2012; 47:61–5. [PubMed: 21720187]
- Tessier FJ, Monnier VM, Sayre LM, Kornfield JA. Triosidines: novel Maillard reaction products and cross-links from the reaction of triose sugars with lysine and arginine residues. *Biochem J.* 2003; 369:705–719. [PubMed: 12379150]
- Thornton IL, Dupps WJ, Roy AS, Krueger RR. Biomechanical effects of intraocular pressure elevation on optic nerve/lamina cribrosa before and after peripapillary scleral collagen cross-linking. *Invest Ophthalmol Vis Sci.* 2009; 50:1227–1233. [PubMed: 18952911]
- Ueno S, Pease ME, Wersinger DMB, Masuda T, Vinoses SA, Licht T, Zack DJ, Quigley H, Keshet E, Campochiaro PA. Prolonged blockade of VEGF family members does not cause identifiable damage to retinal neurons or vessels. *J Cell Physiol.* 2008; 217:13–22. [PubMed: 18543272]
- Watson PG, Young RD. Scleral structure, organization and disease. A review. *Exp Eye Res.* 2004; 78:609–623. [PubMed: 15106941]
- Wiesel TN, Raviola E. Myopia and eye enlargement after neonatal lid fusion in monkeys. *Nature.* 1977; 266:66–68. [PubMed: 402582]
- Wollensak G, Spoerl E, Seiler T. Riboflavin/ultraviolet-A-induced collagen crosslinking for the treatment of keratoconus. *Am J Ophthalmol.* 2003; 135:620–627. [PubMed: 12719068]
- Wollensak G, Iomdina E, Dittert D, Slamatina O, Stoltenburg G. Cross-linking of scleral collagen in the rabbit using riboflavin and UVA. *Acta Ophthalmol Scand.* 2005; 83:477–482. [PubMed: 16029274]
- Wollensak G, Iomdina E. Crosslinking of scleral collagen in the rabbit using glyceraldehyde. *J Cataract Refract Surg.* 2008a; 34:651–656. [PubMed: 18361989]
- Wollensak G, Iomdina E. Long-term biomechanical properties after collagen cross linking of sclera using glyceraldehyde. *Acta Ophthalmol.* 2008b; 86:887–893. [PubMed: 18537936]
- Wollensak G, Iomdina E. Long-term biomechanical properties of rabbit sclera after collagen crosslinking using riboflavin and ultraviolet A (UVA). *Acta Ophthalmol.* 2009; 87:193–198. [PubMed: 18803623]
- Woo SL-Y, Kobayashi AS, Schlegel WA, Lawrence C. Nonlinear material properties of intact cornea and sclera. *Exp Eye Res.* 1972; 14:29–39. [PubMed: 5039845]
- Yang H, Downs JC, Sigal IA, Roberts MD, Thompson H, Burgoyne CF. Deformation of the Normal Monkey Optic Nerve Head Connective Tissue after Acute IOP Elevation within 3-D Histomorphometric Reconstructions. *Invest Ophthalmol Vis Sci.* 2009; 12:5785–5799. [PubMed: 19628739]
- Yang H, Thompson H, Roberts MD, Sigal IA, Downs JC, Burgoyne CF. Deformation of the early glaucomatous monkey optic nerve head connective tissue after acute IOP elevation in 3-D

histomorphometric reconstructions. Invest Ophthalmol Vis Sci. 2011; 52:345–363. [PubMed: 20702834]

### Highlights

- Glyceraldehyde (GA) exposure to the posterior region of the mouse globe had no detectable effects on retina ganglion cells (RGC), retinal structure, or function.
- GA injected eyes endured; an increased cross-linking of sclera by 37%, a decrease of scleral permeability, and an increase in the pressure—strain behavior by *in vitro* inflation testing.
- GA and experimental glaucoma treated eyes had greater IOP and greater RGC loss after 6 weeks compared to naïve and buffer treated eyes.

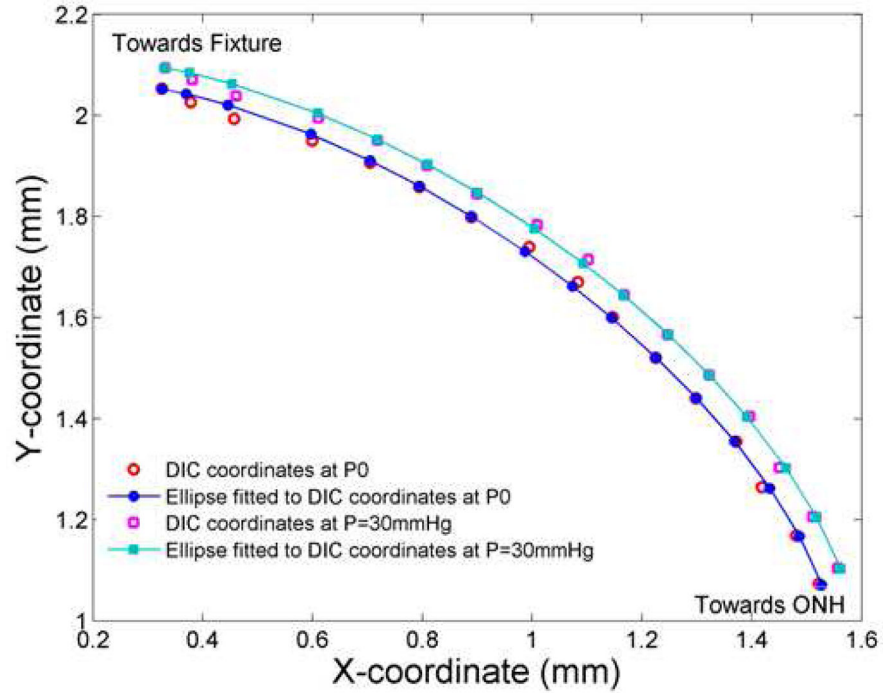


**Figure 1.**

Analysis of scleral inflation data

X and Y DIC coordinates (raw values) are shown from the nasal scleral edge for an eye at  $P_0$  (red circles) and  $P=30$  mm Hg (purple squares). The ellipse fitted points (using DIC values) at  $P_0$  (filled blue circles and line) and deformed positions at  $P=30$  mm Hg for the same eye (teal squares and line). The comparison of raw data points and the fitted ellipse show the modest degree of smoothing that occurred (see Section 2.4. Biomechanical Inflation Testing).

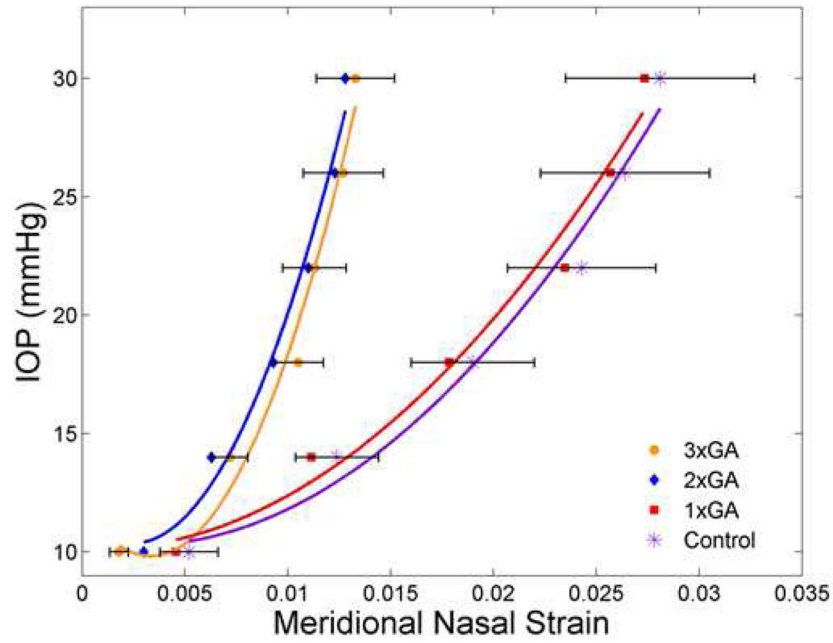


**Figure 2.**

Comparison of IOP—strain for GA-treated and control sclera

The mean IOP—strain values are plotted for 4 groups of mice with loading from reference IOP to 30 mm Hg. The groups are Control (purple asterisk) and 1x treatment with GA (red square) at the right and 2x treatment with GA (blue diamond) and 3x treatment with GA (orange circle) at the left. Standard error bars are shown for control and 3x GA groups. The fitted lines have also been added (for each group) in each respective color. Data from the nasal meridional analysis (temporal meridional and circumferential analyses gave similar results) show the significant stiffening effect after either 2 or 3 treatments with GA.

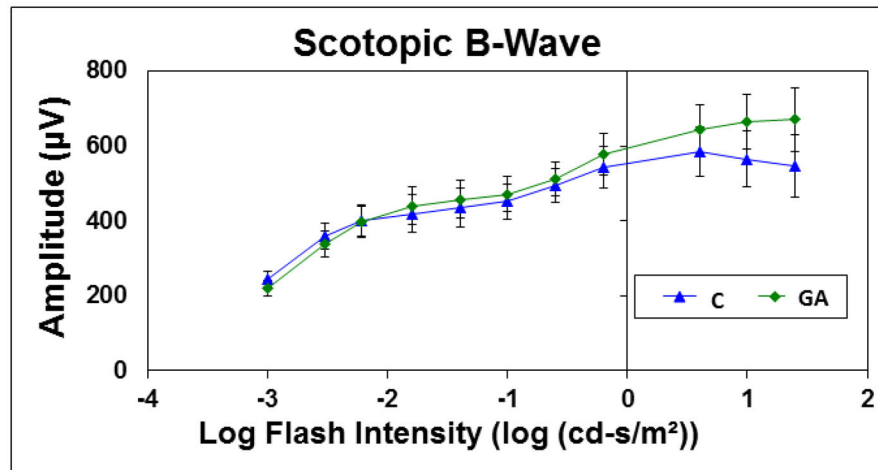


**Figure 3.**

Electroretinogram data for Scotopic B-Wave

The graph plots the mean amplitude for control (blue triangles, N=5) and glycerinaldehyde treated eyes (green diamonds, N=5) at 10 different scotopic, B-wave, flash intensities (amplitudes in µV (microvolts)).

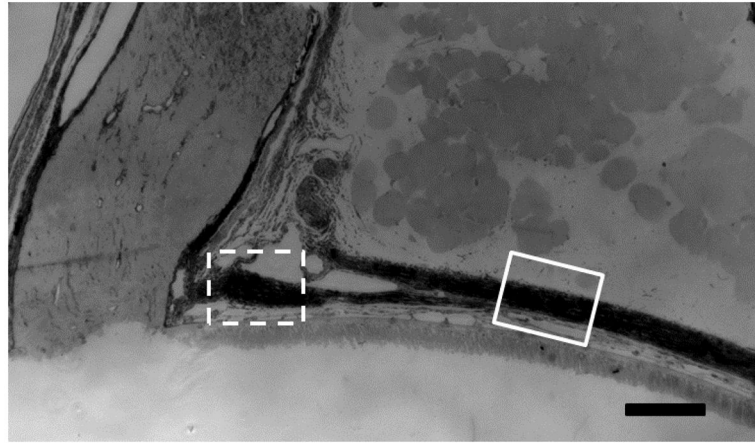


**Figure 4.**

Mouse peripapillary scleral area

The mouse peripapillary sclera, optic nerve head, and optic nerve in epoxy section. The sclera divides into two portions, one splitting off posteriorly to join the dura mater and one continuing directly to the ONH. We measured the scleral thicknesses in two areas, one just prior to the division, which is referred to as the outer peripapillary scleral thickness (solid line square) and one after the division, next to the optic nerve head, referred to as the inner peripapillary sclera (dotted line square; scale bar =100 $\mu$ m).

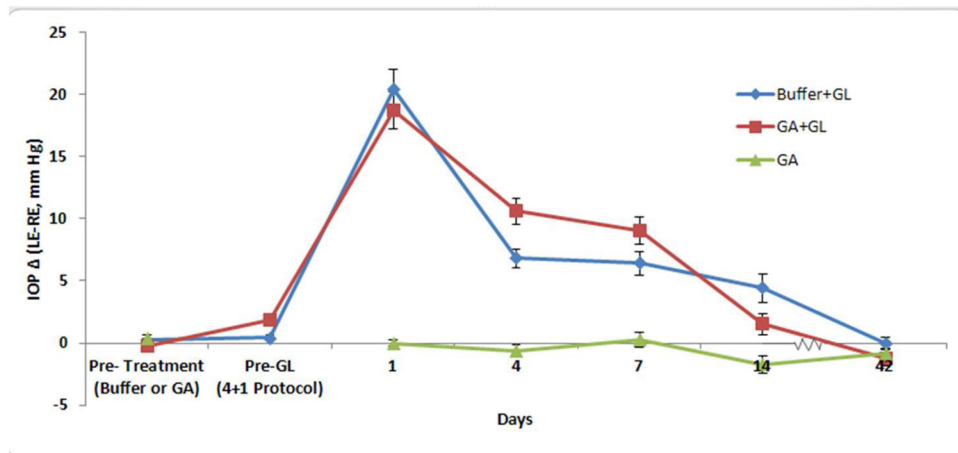


**Figure 5.**

IOP Difference for Buffer+GL, GA+ GL and GA groups

Mean paired IOP difference between left eyes (treated) and right eyes (control) of each animals. From glaucoma experiment 1, the buffer-injected (blue diamonds, N=41) and GA-injected (red squares, B=40) show no significant increase pre-glaucoma (GL) induction after their subconjunctival injection sequences (both  $p > 0.4$ ). After glaucoma induction both GA and buffer groups have significant elevations through the first 2 weeks ( $p < 0.0001$ ), but no significant difference between the two experimental groups (all  $p > 0.27$ ). Animals that were injected with GA alone, but without glaucoma induction had no change in IOP (at either 1, 4, 7, 14 or 42 days) in their injected compared to control eyes (green triangles, N=10). Mean paired difference  $\pm$  standard error.

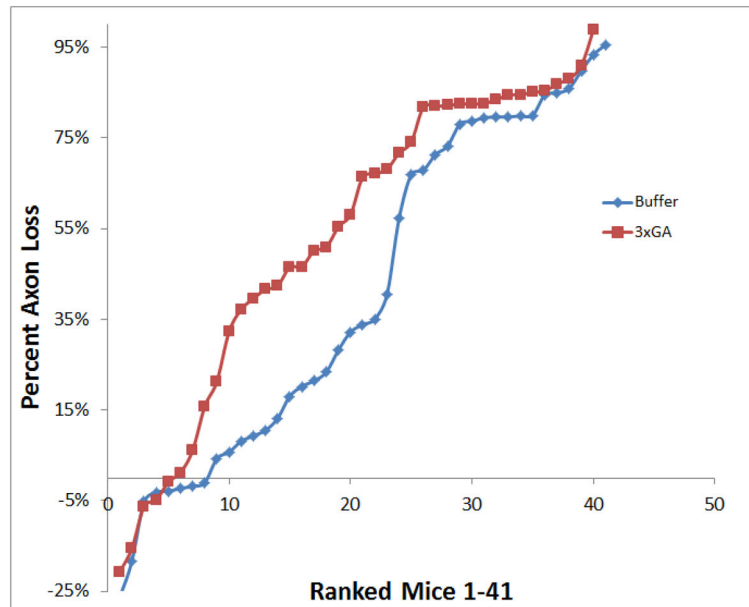


**Figure 6.**

Distribution of RGC axon loss of individual eyes in first glaucoma experiment

This graph plots the distribution of RGC axon loss for each individual mouse by group; 3 times treated GA eyes are represented in red squares (N=1–41) and the buffer injected eyes are represented in blue diamonds (N=1–40). Each eye (numbered 1–41) is ranked in ascending order of percent axon loss, and is plotted to show the distribution of axon loss in each experimental group; 3x GA eyes showed greater amount of axon loss in the 10–60% range when compared to buffer-injected controls.

**Table 1**

Sclera Strain Analysis for Control and 3x GA Injected Animals.

Analysis of Controls, N=28		
Global Ellipse Meridional Strain-Temporal	Mean	Stdev
P10	0.0042	0.0047
P14	0.0112	0.0083
P18	0.0176	0.0104
P22	0.0225	0.0125
P26	0.0254	0.0143
P30	0.0262	0.0152
Global Ellipse Meridional Strain-Nasal		
P10	0.0052	0.0075
P14	0.0124	0.0107
P18	0.0190	0.0158
P22	0.0243	0.0191
P26	0.0264	0.0217
P30	0.0281	0.0243
Circumferential Strain-R1		
P10	0.0063	0.0037
P14	0.0126	0.0070
P18	0.0184	0.0081
P22	0.0233	0.0112
P26	0.0265	0.0151
P30	0.0287	0.0180
Circumferential Strain-R2		
P10	0.0053	0.0043
P14	0.0114	0.0074
P18	0.0174	0.0084
P22	0.0221	0.0105
P26	0.0249	0.0120
P30	0.0264	0.0132
Circumferential Strain-R3		
P10	0.0046	0.0040
P14	0.0102	0.0063
P18	0.0155	0.0076
P22	0.0199	0.0083
P26	0.0225	0.0091
P30	0.0238	0.0096
Circumferential Strain-R4		
P10	0.0044	0.0039

Analysis of Controls, N=28		
Global Ellipse Meridional Strain-Temporal	Mean	Stdev
P14	0.0096	0.0059
P18	0.0145	0.0070
P22	0.0191	0.0076
P26	0.0219	0.0085
P30	0.0234	0.0092

Analysis of 3x GA, N=12				
Global Ellipse Meridional Strain-Temporal	Mean	Stdev	Percent Decrease	p-value
P10	0.0027	0.0037		
P14	0.0065	0.0092		
P18	0.0112	0.0108		
P22	0.0148	0.0122		
P26	0.0163	0.0137		
P30	0.0174	0.0158	34%	p=0.11
Global Ellipse Meridional Strain-Nasal				
P10	0.0018	0.0023		
P14	0.0073	0.0041		
P18	0.0094	0.0052		
P22	0.0104	0.0064		
P26	0.0111	0.0079		
P30	0.0132	0.0081	53%*	p=0.05
Circumferential Strain-R1				
P10	0.0029	0.0016		
P14	0.0089	0.0029		
P18	0.0111	0.0042		
P22	0.0125	0.0048		
P26	0.0140	0.0050		
P30	0.0136	0.0054	53%*	p=0.007
Circumferential Strain-R2				
P10	0.0028	0.0020		
P14	0.0078	0.0046		
P18	0.0107	0.0056		
P22	0.0127	0.0071		
P26	0.0138	0.0075		
P30	0.0151	0.0077	43%*	p=0.0086
Circumferential Strain-R3				
P10	0.0027	0.0020		
P14	0.0077	0.0042		

Analysis of 3x GA, N=12				
Global Ellipse Meridional Strain-Temporal	Mean	Stdev	Percent Decrease	p-value
P18	0.0102	0.0053		
P22	0.0121	0.0062		
P26	0.0132	0.0064		
P30	0.0143	0.0066	40%*	p=0.003
Circumferential Strain-R4				
P10	0.0024	0.0018		
P14	0.0072	0.0038		
P18	0.0096	0.0050		
P22	0.0116	0.0062		
P26	0.0129	0.0066		
P30	0.0139	0.0071	41%*	p=0.0031

GA=glyceraldehyde N= sample size, Mean= mean strain at each pressure, stdev= standard deviation, R1–R4= region along sclera edge (R1- peripapillary region and R4- closest to equator), P10–P30= pressure reading in mm Hg, percent decrease= decrease in strain comparing the control to 3XGA at pressure of 30 mm Hg, p-value= analysis comparing strain of control and 3xGA inflation tested tissue, at each region and for multiple pressures (during the load).

\* These are not Bonferroni corrected p-values, however, the circumferential strains meet the p=0.009 significance criterion for Bonferroni correction with 6 tests.

Table 2

## Experimental Groups

Experiment	N	Purpose of Study*	Control <sup>†</sup>	GA	GA + GL	GL	Buffer + GL	Buffer	GA Soaked	Weeks Followed
Glaucoma Experiment 1	81	Effect of GA on glaucoma-induced damage			40		41			7
Glaucoma Experiment 2	50	Effects of GA on glaucoma damage and scleral thickness		10	20	20				7
IOP Calibration	6	Quality of IOP readings on Injected eyes	3	3						7
Retina Histology	5	Effect of GA on retinal tissue		5						7
ERG	5	Effect of GA on photopic and scotopic retinal function		5						7
AGE	37	Effect of GA on cross-linking	5	13				14	5	7
FRAP	39	Effect of GA on sclera permeability	19	10	10					7
Inflation/Stiffness	157	Effect of GA on stress/strain	28	23	31	20	28		26	7

\* Animals received treatment on le4 eyes, while right eyes were untreated.

<sup>†</sup> Control animals were bilateral naive controls.

GA = glycerinaldehyde; GL = glaucoma induced via bead model. Weeks Followed = 7 weeks total (1 week of “stiffening” treatment and 6 weeks of glaucoma treatment)

**Table 3**

Retinal layer thickness in GA and control mice

	Control (N=5)		GA injected (N=5)		% Diff
	Mean $\pm$ stdev	Median	Mean $\pm$ stdev	Median	
Inner nuclear layer	42.8 $\pm$ 2.5	42.9	42.7 $\pm$ 4.1	43.3	-1.1 *
Outer nuclear layer	57.2 $\pm$ 8.7	55.7	57.4 $\pm$ 4.0	58.6	0.4 *

\* p = 0.9, t tests; data in micrometers; stdev = standard deviation, GA = glycerinaldehyde treated, diff = difference.

**Table 4**

Histological peripapillary scleral thickness

Location	N	Control	GA	GA + GL	GA
Outer Sclera	5	32.7 ± 2.3	37.0 ± 9.7	39.0 ± 4.4	41.3 ± 3.3
Inner Sclera	5	37.5 ± 2.8	38.8 ± 9.6	45.5 ± 3.6	49.1 ± 7.4

mean ± standard deviation; micrometers; GA=glyceraldehyde; GL= glaucoma induced via bead model.

**Table 5**

FRAP half time to recovery data

Location	Control		GA		GA + GL	
	N	t½	N	t½	N	t½
All 3 zones	57	2.21 ± 1.22	30	2.65 ± 1.30*	30	2.56 ± 1.54†
Peripapillary	20	3.33 ± 1.01‡	10	3.65 ± 1.30^	10	4.19 ± 1.56^
0.75 mm	20	1.52 ± 0.42	10	2.09 ± 0.62	10	1.51 ± 0.56
1.50 mm	20	1.81 ± 1.01	10	2.52 ± 1.36	10	2.23 ± 0.82

\* difference from control: p = 0.001;

† difference from control: p = 0.24;

GA = glycerinaldehyde; GL = glaucoma induced via bead model;

‡ difference of control peripapillary from other two control zones both p < 0.001;

^ difference from control of GA and GA+GL in peripapillary area, p = 0.20 and 0.049, respectively. N = samples per group, t½ in minutes; mean ± standard deviation.

**Table 6**

Axial length and width increase in GA and buffer-injected eyes, glaucoma experiment 1

Treatment	N	Length Increase		Width Increase	
		Mean $\pm$ stdev	Median	Mean $\pm$ stdev	Median
GA + GL	40	7.7 $\pm$ 5.6%	6.8%	4.5 $\pm$ 6.6%	3.2%
Buffer + GL	41	10.5 $\pm$ 7.0%	10.1%	6.4 $\pm$ 6.7%	5.2%

GA= glycerinaldehyde; GL= glaucoma induced via bead model; N= samples per group; Mean  $\pm$  standard deviation,.

**Table 7**

Results of glaucoma experiment 2

	N	IOP Measures		Axial Length			Number of Axons		% Loss (pooled control)
		Total Integral	Positive Integral	RE (mm)	LE (mm)	% Difference	RE	LE	
<b>GA</b>									
Mean ± STDEV	10	-44.7 ± 89.7	17.6 ± 41.4	3.6 ± 0.1	3.6 ± 0.1	1.8 ± 4.2	61,256 ± 4,945	60,775 ± 3,903	0.8 ± 6.4
Median	10	-21	11	3.6	3.6	0.0%	61,616	61,111	0.2%
<b>GA + GL</b>									
Mean ± STDEV	20	169.4 ± 275.7	200.5 ± 250.6	3.6 ± 0.2	3.8 ± 0.3	8.9 ± 11.0	57,247 ± 9,102	31,710 ± 18,522	44.6 ± 32.4
Median	20	141	149	3.5	3.9	<b>7.0%<sup>‡</sup></b>	60,474	32,285	<b>43.6%<sup>‡</sup></b>
<b>GL</b>									
Mean ± STDEV	20	184.3 ± 196.6	194.7 ± 183.2	3.6 ± 0.1	3.7 ± 0.5	2.8 ± 12.5	60,608 ± 5,087	46,642 ± 18,731	23.0 ± 30.9
Median	20	139	133	3.6	3.9	7.9%	60,555	49,488	<b>18.3%<sup>‡</sup></b>
P-value		diff GA alone vs. GA + Bead	<b>0.03</b>	0.095	0.05	0.12	0.11	<b>0.0008</b>	<b>0.002</b>
P-value		diff Glaucoma: GA vs. no GA	0.85	0.71	0.15	0.13	0.17	<b>0.02</b>	<b>0.049</b>

% Difference from fellow eye;

\* p 0.05,

<sup>‡</sup> p 0.01,

<sup>‡</sup> p 0.0001, GA = glycerinaldehyde, GL = glaucoma induced via bead model;

N = sample size; IOP in mm Hg; Total Integral IOP = the cumulative difference in area under the IOP versus time curve between treated eye and control eye IOP; Positive Integral IOP = cumulative difference in area under the IOP versus time curve between the treated eye (LE- left eye) and control eye (RE- right eye) for all time periods when IOP in the treated eye (LE- left eye) exceeded that in the control eye (RE- right eye) (Cone et al., 2010).